

AFM Measurements of Hydrodynamic Forces Between Deformable Drops: Theory and Comparison with Experiments

Rogério Manica*

Steven L. Carnie,

Derek Y.C. Chan

Particulate Fluids Processing Centre, Department of Mathematics and Statistics

The University of Melbourne, Parkville, VIC 3010, Australia

E-mail: rmanica@ms.unimelb.edu.au, carniesl@ms.unimelb.edu.au, D.Chan@unimelb.edu.au

Raymond R. Dagastine

PFPC, Department of Chemical and Biomolecular Engineering

The University of Melbourne, Parkville, VIC 3010, Australia

E-mail: rrd@unimelb.edu.au.

The Atomic Force Microscope (AFM) has recently been used to make direct measurements of the forces involving deformable surfaces such as the interaction between a rigid probe particle and a deformable oil drop across an aqueous electrolyte solution [3]. Dagastine et al. [4] measured the force between two approaching droplets of decane in an aqueous solution of sodium dodecyl sulphate (SDS) in which one drop (radius $R_c \sim 43\mu\text{m}$ and contact angle θ_c (unknown) but in the range $90^\circ - 180^\circ$) is attached to the AFM cantilever with known spring constant K . The other drop (radius $R_d \sim 90\mu\text{m}$ and contact angle $\theta_d \sim 50^\circ$) is attached to a piezoelectric stage that is moved according to a programmed velocity schedule. The stage is moved towards the cantilever with constant velocity V over a displacement ΔX_{max} and is then reversed over the same distance while the deflection of the spring is recorded and converted to a force F using the spring constant of the cantilever. Therefore, the experimental data consist of values of the piezoelectric stage position X and the corresponding force F .

A characteristic feature seen in the measured forces between decane drops [4] is the dependence on the approach velocity V . At low velocities, the force law is reversible, being the same on approach and retract, with an approximately constant compliance region. At higher velocities that are comparable to velocities due to thermal motion of drops in a suspension, the force curves show hysteresis. Attractive forces of significant magnitude are observed in the retract phase of the programmed velocity schedule.

The experimental parameters are summarized in Table 1. All parameters are explained in the text when they are needed.

The drops size, interfacial tension, and approach velocities (about 10 microns/s) are in a regime

Type	Physical parameter	Value
Surface force	Surface potential, ψ_0	-100 mV
	Concentration, n	3 mM SDS
Fluid	Viscosity (water), μ	0.89 mPa s
	Surface tension, σ	17.5 mN/m
	Radius cantilever, R_c	$\sim 43 \mu\text{m}$
	Radius piezo, R_d	$\sim 90 \mu\text{m}$
	Contact angle p, θ_d	50°
	Contact angle c, θ_c	$90^\circ - 180^\circ$
AFM	Spring constant, K	0.12 N/m
	Piezo travel, ΔX_{max}	2.0 μm
	Velocity, V	2-28 $\mu\text{m/s}$
	Separation, h_0	$\sim 1.8 \mu\text{m}$

Table 1: Experimental parameters of the drop-drop interaction in an AFM.

where surface forces, hydrodynamic effects and drop deformation are all significant. A theoretical model taking into account as well as AFM cantilever deflection has been developed. Using matched asymptotic expansions, a new boundary condition for moving drops under AFM experimental conditions has been derived. This boundary condition is necessary to obtain results that are independent of the size of the computational domain.

Figure 1 shows a scheme of the experiments performed by Dagastine et al. [4]. In the scheme, we used symmetric drops for which the theory was originally derived; the drops are actually different but of the same material. The deduction of the governing equations was published in Carnie et al [2] and a summary of the final set is presented. For details, see the paper.

The time evolution of the thickness of liquid film between the two liquid drops is:

$$\frac{\partial h}{\partial t} = \frac{1}{12\mu r} \frac{\partial}{\partial r} \left(r h^3 \frac{\partial p}{\partial r} \right) \quad (1)$$

where $h(r, t)$ is the film thickness as a function of

*Supported by a University of Melbourne International Research Scholarship

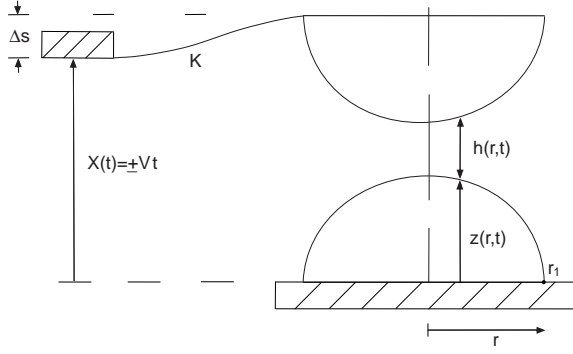


Figure 1: Schematic of two drops approaching each other in AFM

radial coordinate r and time t , $p(r, t)$ is the excess hydrodynamic pressure in the film relative to the bulk liquid, μ is the film viscosity (assumed Newtonian). Note that thin film theory was assumed as well as no-slip boundary condition between the water and the oil drops.

For the pressure, we use the Young-Laplace equation, which comes from a minimization of the drop surface energy in the presence of external forces, subject to a constant volume (incompressibility) constraint.

$$p + \Pi = \frac{2\sigma}{R} - \frac{\sigma}{2r} \frac{\partial}{\partial r} \left(r \frac{\partial h}{\partial r} \right) \quad (2)$$

where σ is the interfacial tension of the drop-film surface, R is harmonic mean ($R^{-1} = R_c^{-1} + R_d^{-1}$) of the unperturbed radius of the drops. $(2\sigma/R)$ is the Lagrange multiplier associated with the constant drop volume constraint and Π is the disjoining pressure. In the experiments of [4], a layer of adsorbed negatively charged surfactant on the drops produces a repulsive double layer disjoining pressure of the form [5]

$$\Pi(h) = 64nkT \tanh^2(e\psi_0/4kT) \exp(-\kappa h(r, t)) \quad (3)$$

which depends on the surface potential ψ_0 of the drops, being $\kappa = \sqrt{2ne^2/\epsilon kT}$ the usual Debye-Hückel parameter that depends on salt concentration n .

The initial condition assumes a parabolic surface in the drops depending on the unperturbed radius and is written as

$$h(r, 0) = h_0 + \frac{r^2}{R} \quad (4)$$

where h_0 is the initial separation between the drop, which is unknown in the experiment, but can be obtained accurately using the theory. The boundary conditions are

$$\frac{\partial h}{\partial r} = 0 \text{ at } r = 0 \quad (5)$$

$$\frac{\partial p}{\partial r} = 0 \text{ at } r = 0 \quad (6)$$

$$p = 0 \text{ for } r = r_{max} \quad (7)$$

$$\dot{h} + \mathcal{F}\dot{G} = \mp V \text{ for } r = r_{max} \quad (8)$$

where \mathcal{F} is

$$\mathcal{F} = 2 + \ln \left(\frac{r_{max}^2}{4R^2} \right) + \ln \left(\frac{1 + \cos \theta}{1 - \cos \theta} \right) - \frac{2\pi\sigma}{K} \quad (9)$$

for the fixed (or stick) contact line case, being θ the contact angle of the *undeformed* drop at the piezo stage. For the case where the contact angle θ_p is fixed, while the three-phase contact line can slip during interaction, \mathcal{F} becomes

$$\mathcal{F} = 2 + \ln \left(\frac{r_{max}^2}{4R^2} \right) + \ln \left(\frac{1 + \cos \theta_{p1}}{1 - \cos \theta_p} \right) - \frac{2}{2 + \cos \theta_p} - \frac{2\pi\sigma}{K} \quad (10)$$

The quantity G is related to the force F between the drops by

$$G = \frac{F}{2\pi\sigma} = \frac{1}{\sigma} \int_0^\infty r[p(r, t) + \Pi(h(r, t))] dr \quad (11)$$

We use the following scales [6]

$$h_c = R_0 C a^{1/2}$$

$$r_c = R_0 C a^{1/4}$$

$$p_c = \sigma/R_0$$

$$t_c = \mu C a^{-1/2}/p_c$$

where $C a = \frac{\mu V}{\sigma}$ is the capillary number (the ratio of viscous forces to surface tension forces) to produce the non-dimensional form of the equations, leading for example to the boundary conditions

$$p = 0 \quad \text{and} \quad \frac{\partial h}{\partial t} + \frac{dG}{dt} \mathcal{F} = \mp 1 \quad \text{at } r = r_{max} \quad (12)$$

where

$$\mathcal{F} = 2 + \ln \left(\frac{r_{max}^2 \sqrt{C a}}{4} \right) + \ln \left(\frac{1 + \cos \theta}{1 - \cos \theta} \right) - \frac{2\pi\sigma}{K} \quad (13)$$

if the position of the three-phase contact line of the drop is fixed. For the constant contact angle boundary condition $\theta = \theta_p$ (fixed)

$$\mathcal{F} = 2 + \ln \left(\frac{r_{max}^2 C a^{1/2}}{4} \right) + \ln \left(\frac{1 + \cos \theta_p}{1 - \cos \theta_p} \right) - \frac{2}{2 + \cos \theta_p} - \frac{2\pi\sigma}{K} \quad (14)$$

We use central differencing in r to obtain a system of differential equations for $h_j(t) \equiv h(j\Delta r, t)$, $j = 0 \dots N$ where $N = r_{max}/\Delta r$. A uniform grid in $r = [0, r_{max}]$ is used with $\Delta r = 0.05$ and $r_{max} = 15$

producing a system of 300 equations. The boundary conditions at $r = 0$ are used to produce the equation for \dot{h}_0 and Eq. (12) provides the equation for \dot{h}_N . This requires G as an extra variable to solve for. The functional G is obtained by evaluating the following integral using Simpson's rule

$$G = \frac{1}{\sigma} \int_0^{r_{max}} r[p(r,t) + \Pi] dr$$

which relates G to all the other variables h_j as an algebraic constraint.

In summary, the final system of equations has the form

$$\begin{pmatrix} 1 & 0 & \cdots & 0 & 0 \\ 0 & 1 & 0 & \cdots & 0 \\ & & \vdots & & \\ 0 & 0 & \cdots & 1 & \mathcal{F} \\ 0 & 0 & \cdots & 0 & 0 \end{pmatrix} \begin{pmatrix} \dot{h}_0 \\ \dot{h}_1 \\ \vdots \\ \dot{h}_N \\ \dot{G} \end{pmatrix} = \begin{pmatrix} f_0 \\ f_1 \\ \vdots \\ \mp 1 \\ \zeta \end{pmatrix} \quad (15)$$

where $\zeta = G - \sum_j w_j g(h_j)$ and f_j represent the discretized contributions of the thinning equation and normal stress balance. This system has a singular mass matrix and is a differential-algebraic equation (DAE) of index 1. It can be solved by standard software, in our case Matlab's `ode15s`.

A comparison between theory and experiment is given in Figure 2. The agreement is impressive across the range of velocities of the experiment. The top figure shows the best fit that can be achieved within experimental error. The various physical parameters of the system in Table 1 have inherent experimental uncertainty. The combined effects of possible theoretical calculation of Force *vs* Extension are indicated as a grey band in the lower figure.

Recent tests using the same model for a different system also show excellent agreement between this theory and the experiments. We hope to be able to explain the interaction between droplets in real systems such as emulsions and flotation processes, helping the development of more stable systems.

References

- [1] D.C. Bardos, Contact angle dependence of solid probe-liquid drop forces in AFM measurements, *Surface Science*, 515 (2002) 157-176.
- [2] S.L. Carnie, D.Y.C. Chan, C. Lewis, R. Manica, R.R. Dagastine, Measurement of dynamical forces between deformable drops using the Atomic Force Microscope. I. Theory *Langmuir*, 21 (2005) 2912-2922.
- [3] D.Y.C. Chan and R.R. Dagastine and L.R. White, Force between a rigid probe particle and a liquid interface I. The repulsive case, *Journal of Colloid and Interface Science*, 236 (2001) 141-154.

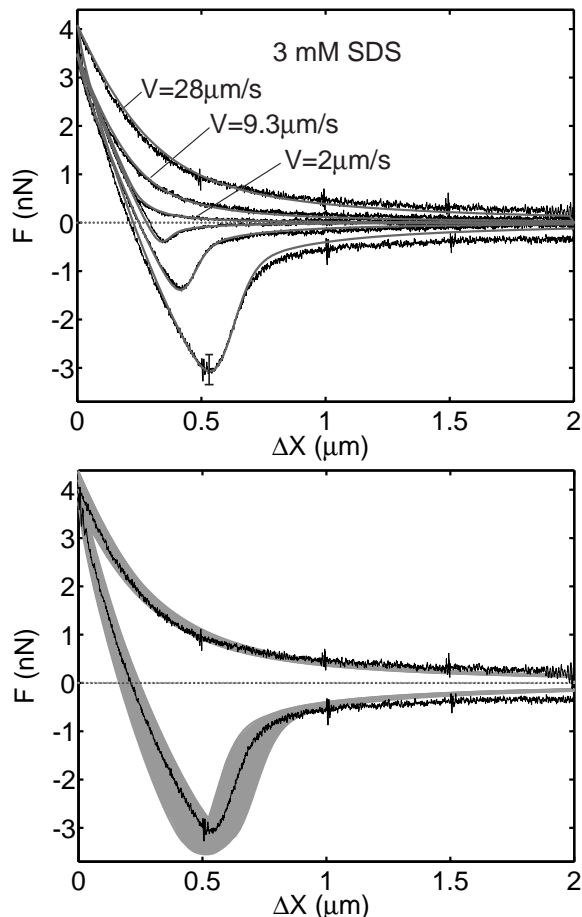


Figure 2: Theory and experiment for $V=2, 9.3$ and $28 \mu\text{m/s}$ and 3 mM SDS concentrations. Top figure shows the best fit and bottom a band representing all the solutions that can be obtained within experimental error

- [4] R.R. Dagastine and G.W. Stevens and D.Y.C. Chan and F. Greiser, Forces between two oil drops in aqueous solution measured by AFM, *Journal of Colloid and Interface Science*, 273 (2004) 339-342.
- [5] R.J. Hunter, "Foundations of Colloid Science", Clarendon Press, 1986, Vol. 1.
- [6] E. Klaseboer and J.Ph. Chevallier and C. Gourdon and O. Masbernat, Film drainage between colliding drops at constant approach velocity: experiments and modeling, *Journal of Colloid and Interface Science*, 229 (2000) 274-285.